Eur. Phys. J. D **1**, 259-264 (1998)

THE EUROPEAN PHYSICAL JOURNAL D

Energy pooling in caesium vapour: $Cs^*(6P_J) + Cs^*(6P_{J'}) \rightarrow Cs(6S) + Cs^{**}(6D)$

C. Vadla[a]

Institute of Physics, Bijenicka 46, 10000 Zagreb, Croatia

Received: 10 June 1997 / Revised: 13 October 1997 / Accepted: 5 January 1998

Abstract. The total rate coefficient k for the energy pooling process $Cs^*(6P) + Cs^*(6P) \rightarrow Cs(6S) + Cs^{**}(6D)$ has been measured in dependence on the ratio of the number densities of the Cs 6P fine-structure sublevels. The measurements were performed applying the laser fluorescence method. From the set of the obtained data for k, the rate coefficients for the particular $Cs^*(6P_J) + Cs^*(6P_{J'})$ collisions were derived. The obtained values for the $Cs^*(P_{1/2}) + Cs^*(P_{1/2})$, $Cs^*(P_{1/2}) + Cs^*(P_{3/2})$ and $Cs^*(P_{3/2}) + Cs^*(P_{3/2})$ collisions at $T = 600$ K are $k_1 = 2 \times 10^{-9}$ cm^3 s^{-1}, $k_2 = 3.1 \times 10^{-10}$ cm^3 s^{-1} and $k_3 < 3 \times 10^{-10}$ cm^3 s^{-1}, respectively. The value for k_1 and the estimate for k_3 are consistent with the data previously published by other authors. The rate coefficient k_2 is reported for the first time.

PACS. 34.50.-s Scattering of atoms, molecules, and ions – 32.00 Atomic properties and interactions with photons

1 Introduction

Recently, two experimental investigations on energy pooling (EP) processes in caesium vapours have been published [1,2]. Among the other EP collisions, in both works the reaction

$$Cs^*(6P) + Cs^*(6P) \rightarrow Cs(6S) + Cs^{**}(6D) \qquad (1)$$

was studied too. This process is known as the first ever observed EP process, which was reported by Klyucharev and Lazarenko [3] 25 years ago. An appropriate steady-state rate equation for the reaction (1) can be written as

$$\frac{\mathrm{d}}{\mathrm{d}t}N(6D) = 0 = \frac{k}{2}N^2(6P) - \frac{N(6D)}{\tau_{6D}} \qquad (2)$$

where k is the EP rate coefficient and τ_{6D} is the radiative lifetime of the 6D state. The factor 1/2 in equation (2) prevents double counting of each colliding pair of identical particles in a closed cell. This factor, introduced by Bezuglov *et al.* [4] becomes important when the results of experiments in a closed cell are compared with the beam experiments and theoretical results for the corresponding cross sections.

The authors in reference [3] estimated the upper value for the cross section for the process (1), $\sigma = k/v^{\mathrm{rel}}_{\mathrm{Cs-Cs}}$, to be about 10^{-13} cm^2 at $T = 530$ K. A theoretical study made by Borodin and Komarov [5] established that this cross section should be in the range between 1.5×10^{-15} cm^2 and 2×10^{-14} cm^2 at $T = 500$ K. The process inverse to (1) has been investigated by Yabuzaki *et al.* [6] and the measured cross section at $T = 500$ K was found to be 1.5×10^{-14} cm^2. The authors in reference [1] reported the rate coefficient $k/2 = 4.2 \times 10^{-10}$ cm^3 s^{-1} at $T = 570$ K for the process (1). Using the principle of detailed balancing, this datum was found to be consistent with the result given in [6]. Jabbour *et al.* [2] investigated the J-selective $Cs^*(6P_{1/2}) + Cs^*(6P_{1/2})$ and $Cs^*(6P_{3/2}) + Cs^*(6P_{3/2})$ collisions. Their results, compared with the results obtained in this work, are listed in Table 1.

The measurements of the J-selective EP rate coefficients are important because the obtained experimental data can be used as a sensitive check for the calculated interaction potentials between the colliding particles. On the other hand, the information about the EP collisions is of great interest for recent cooling and trapping experiments, since such collisional processes can produce a significant contribution to the trap losses. The results presented here were obtained at relatively high temperatures. However, these results, combined with the results of the previous measurements, might be useful for determination of the EP rate coefficients temperature dependence.

The rate coefficient k in equation (2) is related to the total number density $N(6P) = N(P_{1/2}) + N(P_{3/2})$ of the caesium first resonance state and to the total number density $N(6D) = N(6D_{3/2}) + N(6D_{5/2})$ of the final EP state 6D. Regarding the fine structure of the 6P state, the rate coefficient k comprises three particular contributions k_1, k_2 and k_3, which correspond to the

[a] e-mail: vadla@ifs.hr

Table 1. The values for the rate coefficients and the corresponding cross sections for the processes $Cs^*(6P_J) + Cs^*(6P_{J'}) \rightarrow Cs(6S) + Cs^{**}(6D)$ measured here and by Jabbour *et al.* [2]. The experimental errors for the data obtained in this work are 40% and 80% for k_1 and k_2, respectively. The accuracy of the values of Jabbour *et al.* [2] is about 30%. For further comments see the text.

EP collision pair	This work ($T = 600$)		Reference [2] ($T = 340$)	
	k_i (10^{-10} cm^3/s)	σ_i (10^{-16} cm^2)	k_i (10^{-10} cm^3/s)	σ_i (10^{-16} cm^2)
$Cs^*(6P_{1/2}) + Cs^*(6P_{1/2})$	20	440	7.1	210
$Cs^*(6P_{1/2}) + Cs^*(6P_{3/2})$	3.1	70	-	-
$Cs^*(6P_{3/2}) + Cs^*(6P_{3/2})$	< 3	< 70	2.8	83

$Cs^*(6P_{1/2}) + Cs^*(6P_{1/2})$, $Cs^*(6P_{1/2}) + Cs^*(6P_{3/2})$ and $Cs^*(6P_{3/2}) + Cs^*(6P_{3/2})$ collisions, respectively. The relation between the total coefficient k and the particular coefficients k_i is given as follows:

$$\frac{k}{2}N^2(6P) = \frac{k_1}{2}N^2(6P_{1/2}) + k_2 N(6P_{1/2})N(6P_{3/2}) + \frac{k_3}{2}N^2(6P_{3/2}). \quad (3)$$

In contrast to the first and third term on the right side of equation (3), the second term describing the collisions between non-identical particles does not include the factor of 1/2. With the substitute $\eta = N(P_{1/2})/N(P_{3/2})$, equation (3) can be rewritten in the following form:

$$\frac{k}{2}(1+\eta)^2 = \frac{k_1}{2}\eta^2 + k_2\eta + \frac{k_3}{2}\cdot \quad (4)$$

In contrast to the the k_i, the total rate coefficient k depends strongly on the value of η. In the present experiment, performed at the constant temperature $T = 600$ K, the quantity $F = \frac{k}{2}(1+\eta)^2$ has been measured relatively as a function of the η. The values of F in absolute scale were determined using the absolute datum for $k/2$ obtained at $T = 570$ K [1]. By fitting the set of the obtained experimental data to the formula (4) the particular coefficients k_i were obtained.

2 Experiment and method

The experiment was performed by cw laser fluorescence method. The experimental set-up is similar to that which was reported in [1]. In contrast to that experiment, which was performed in the heat-pipe, here the caesium vapours were generated in the evacuated cylindrical glass cell (inner diameter: 2 cm, inner length: 13 cm). The temperature of the cell was kept constant at $T = 600$ K, while the temperature of the metal bath in the cell finger was varied in the range between 460 K and 560 K. In this way, the number density of the caesium vapour in the cell was changed between 5×10^{14} cm^{-3} and 1.4×10^{16} cm^{-3}. Similarly as in reference [1], caesium atoms were excited by cw ring dye-laser, tuned to the frequency of the centre of the stronger h.f. component of the $6S_{1/2} \rightarrow 5D_{5/2}$ quadrupole transition. The $6P_J$ states were populated by subsequent relaxation of the directly excited state. In the absence of collisional transfer processes only the $6P_{3/2}$ state is radiatively populated when the $5D_{5/2}$ state is excited. Due to the collisions with caesium ground state atoms the collisional intramultiplet and intermultiplet mixing of the 5D and 6P states occurs. Consequently, this gives a raise to the $6P_{1/2}$ population due to the collisional $6P_{3/2} \rightarrow 6P_{1/2}$ and $5D \rightarrow 6P_{1/2}$, as well as radiative $5D_{3/2} \rightarrow 6P_{1/2}$ transitions. In thermal equilibrium at $T = 600$ K the ratio $\eta = 1.9$. By variation of the caesium ground state number density a significant change in the $N(P_{1/2})$ to $N(P_{3/2})$ ratio (in principle, between 0 and equilibrium value) can be produced, when $5D_{5/2}$ is optically pumped.

The ring laser beam was split in two parts. The first part, the exciting beam (power: 50 mW; diameter: 0.5 mm) was shone perpendicular to the cell axis at the distance of about 5 mm from the cell window. The fluorescence zone was observed in the cell axis direction and its part (length: 5 mm) was imaged in 1:3 ratio onto the entrance slit of the 1m McPherson monochromator (slit widths: 0.2 mm). The monochromator was supplied by a RCA S-20 photomultiplier. The second, weaker part of the split beam, was used to control the caesium ground state number density N_{Cs} by measuring the peak absorption coefficient of the optically thin Cs quadrupole pump line. At highest caesium number densities $N_{Cs} \approx 10^{16}$ cm^{-3} the Lorentz to Doppler width ratio was found to be less than 0.05, and consequently, the shape of the quadrupole line kernel in the whole range of the investigated caesium number densities could be fairly regarded as a pure Doppler profile. In this case, the peak absorption coefficient $\kappa_0 = N_{Cs}\sqrt{\pi}e^2 f_{nm}/m_e\nu_{mn}\sqrt{2kT/M_{Cs}}$. The oscillator strength of the pumped stronger h.f. component of the $6S_{1/2} \rightarrow 5D_{5/2}$ quadrupole transition amounts to $f^{str}_{685} = (9/16)f^{tot}_{685}$. The caesium ground state number density was determined using the value for the total oscillator strength $f^{tot}_{685} = 5.65\times10^{-7}$ taken from reference [7]. Actually, as shown below, the exact knowledge of the caesium ground state density was not needed for the evaluation of the rate coefficient, since for the application of the method used, the measurement of the pump line peak absorption coefficient was sufficient. The absorption beam passed the cell parallel to its axis. In order to measure the κ_0 (*i.e.*, N_{Cs}) in a wide range, the single, double and triple pass of the absorption beam was applied. After passing the cell, the intensity of the absorption beam was measured by a photodiode.

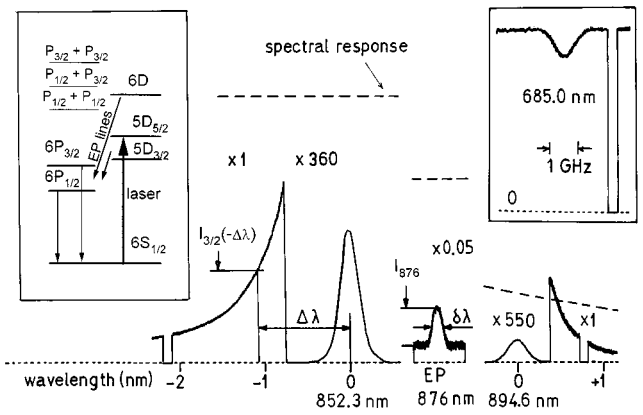

Fig. 1. Typical spectra measured by scanning the monochromator, while the frequency of the pump laser was kept on the centre of the strongest h.f. component of the $6S_{1/2} \rightarrow 5D_{5/2}$ quadrupole transition. The monochromator band-pass was 0.2 nm. The line wing intensities were evaluated in the range between 1 nm (for lower caesium number densities) and 3 nm (for higher caesium number densities). The inset on the left side shows the partial term diagram of caesium together with the relevant transitions. The inset on the right side shows the absorption spectra (double pass through the cell) obtained by scanning the laser across the pump transition.

The fluorescence intensities of the caesium resonance lines and the energy pooling lines 876 nm, 917 nm and 921 nm (6D $\rightarrow$ 6P transitions) were measured by scanning the monochromator, while the frequency of the ring laser was kept on the centre of the pump transition. The typical spectra are displayed in Figure 1.

Alkali resonance line wings can be used as a quasi-continuous relative standard of radiation. As reported in [1], for the wavelength detuning $\Delta\lambda$ from the line centre, the registered intensity of the Cs D_1 red ($+\Delta\lambda$) or Cs D_2 blue ($-\Delta\lambda$) line wing can be described with:

$$I_J(\pm\Delta\lambda) \propto \nu_J \delta\lambda \frac{\beta_J}{(\Delta\lambda)^2} N(\mathrm{P}_J) N_{\mathrm{Cs}} \exp\left[-\frac{hc\Delta\lambda}{\lambda^2 kT}\right]. \quad (5)$$

Here, ν_J is the central frequency of the line and $\delta\lambda$ is the monochromator band-pass. The factors $\beta_{3/2}$ for Cs D_2 and $\beta_{1/2}$ for Cs D_1 line are in the ratio 1.675 [1]. It should be emphasized that (5) is valid if the band pass $\delta\lambda$ is small compared with the detuning $\Delta\lambda$.

The experimental conditions here and in the previous experiment [1] were similar. The number density of the 6P state was about 5×10^{10} cm^{-3}, and the diameter of the fluorescence zone was about 0.5 mm. Under these conditions, the 6D $\rightarrow$ 6P EP transition lines were optically thin and their total intensity I_{EP} was directly proportional to the N(6D).

As mentioned in the Introduction, the aim of the experiment was to utilize equation (4) for the determination of the rate coefficients k_i. To do so, the dependence of the quantity $F = \frac{k}{2}(1+\eta)^2$ on the parameter η had to be obtained, which was done in the following way.

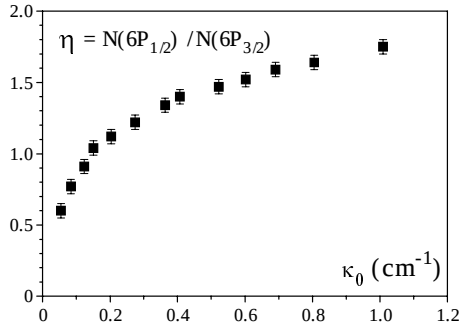

Fig. 2. The ratio $\eta = N(\mathrm{P}_{1/2})/N(\mathrm{P}_{3/2})$ in dependence on the peak absorption coefficient κ_0 of the pumped quadrupole line.

Equation (5) yields the formula for evaluation of the ratio η:

$$\eta = 1.675 \frac{\nu_{3/2}}{\nu_{1/2}} \frac{I_{1/2}(+\Delta\lambda)}{I_{3/2}(-\Delta\lambda)} \exp\left(-\frac{2hc\Delta\lambda}{\lambda^2 kT}\right). \quad (6)$$

For a series of temperatures, the ratio of the intensities of the resonance wings $I_{1/2}(+\Delta\lambda)/I_{3/2}(-\Delta\lambda)$ and the peak absorption coefficient κ_0 of the pumped quadrupole line were measured (Fig. 1). The ratios η were calculated according to equation (6) and their κ_0-dependence is displayed in Figure 2. On the other hand, according to equation (2) and relation (5), the quantity F can be expressed as:

$$F = \frac{k}{2}(1+\eta)^2 \propto \frac{N(\mathrm{6D})}{N^2(\mathrm{6P}_{3/2})} \propto \frac{I_{\mathrm{EP}} N_{\mathrm{Cs}}^2}{I_{3/2}^2(-\Delta\lambda)}. \quad (7)$$

Since the ground state caesium density N_{Cs} is proportional to the peak absorption coefficient κ_0 of the pumped quadrupole line, while the square of the resonance wing intensity in the denominator can be factorized, the expression (7) can be rewritten in the following form:

$$F = \frac{k}{2}(1+\eta)^2 \propto \frac{I_{\mathrm{EP}}}{I_{3/2}(-\Delta\lambda)} \frac{\kappa_0^2}{I_{3/2}(-\Delta\lambda)}. \quad (8)$$

The above expression shows that F as a function of κ_0 (or N_{s}), can be determined by measuring the κ_0-dependence of two factors. The first factor is the EP line to Cs D2 line wing intensity ratio, and the second one is the ratio between the square of the peak absorption coefficient and the intensity in the blue wing of Cs D2 line.

The intensity ratio $I_{\mathrm{EP}}/I_{3/2}(-\Delta\lambda)$ as a function of κ_0 was obtained from the set of the measurements which are illustrated in Figure 1. The $\kappa_0^2/I_{3/2}(-\Delta\lambda)$ *versus* κ_0 dependence was determined by simultaneous measurement of the peak-absorption coefficient of the pumped stronger h.f. component of the 685 nm quadrupole line and the Cs D2 line wing intensity. The typical signals obtained in this part of the experiment are shown in Figure 3. In contrast to the measurement of the intensity ratios $I_{1/2}(+\Delta\lambda)/I_{3/2}(-\Delta\lambda)$ and $I_{\mathrm{EP}}/I_{3/2}(-\Delta\lambda)$, the measurements of the $\kappa_0^2/I_{3/2}(-\Delta\lambda)$ can be influenced by the change of the cell window transparency. Namely, for determination of the latter quantity, the intensity $I_{3/2}(-\Delta\lambda)$

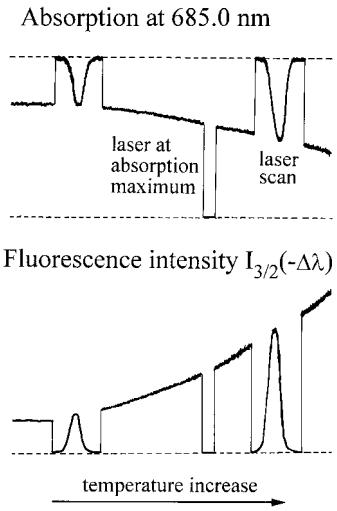

Fig. 3. Typical signals obtained by the simultaneous measurement of the pump line peak-absorption (single pass through the cell) and the Cs D_2 resonance line wing intensity, while the temperature of the cell finger, *i.e.*, the caesium ground state number density in the cell was increased. In this measurement the frequency of the laser was tuned to the centre of the strongest h.f. component of the $6S_{1/2} \rightarrow 5D_{5/2}$ quadrupole transition. The fluorescence intensity in the blue wing of the Cs D_2 line was monitored by the monochromator adjusted at the detuning $\Delta\lambda = 1.5$ nm. During the measurement the stability of the laser frequency was checked by periodical laser scans across the pump line.

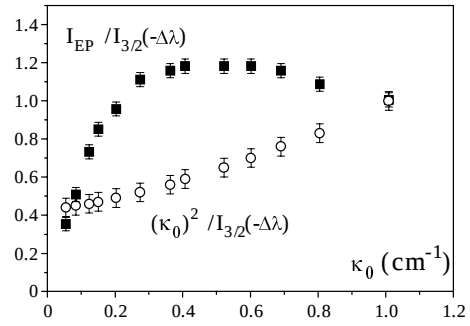

Fig. 4. The $I_{\rm EP}$ to $I_{3/2}(-\Delta\lambda)$ ratio and the $(N_{\rm Cs})^2$ to $I_{3/2}(-\Delta\lambda)$ ratio in dependence on the peak absorption coefficient κ_0 of the pumped quadrupole line. The displayed error bars are due to uncertainties of the laser absorption and fluorescence measurements. The values are normalised to unity for $\kappa_0 = 1$ cm^{-1}.

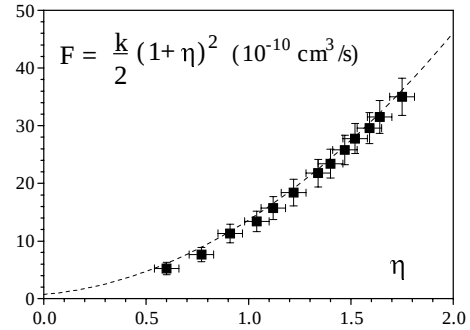

Fig. 5. The absolute values for quantity $F = \frac{k}{2}(1+\eta)^2$ as a function of the ratio η. The dashed line represents the best second order polynomial fit through the experimental data. The displayed error bars comprise the uncertainties depicted in Figures 2 and 4. The determination of the polynomial coefficients is described in the text.

should be measured as a function of κ_0. As one can see from equation (8), for this purpose the $I_{3/2}(-\Delta\lambda)$ can be measured in arbitrary intensity units. However, such a measurement requires, among other things, the constant (or controlled) cell window transparency in the whole caesium density range. The change of the cell window transparency, caused by caesium deposition on the cell walls, was controlled by the white light absorption at 830 nm. It was found that at the highest number densities the transparency was lowered for about 5%. In Figure 4, the data for $I_{\rm EP}$ to $I_{3/2}(-\Delta\lambda)$ ratio, together with the data for $\kappa_0^2/I_{3/2}(-\Delta\lambda)$ are plotted against κ_0. The ratios $I_{\rm EP}/I_{3/2}(-\Delta\lambda)$ and $\kappa_0^2/I_{3/2}(-\Delta\lambda)$ were both normalised to unity for $\kappa_0 = 1$ cm^{-1}.

From the results displayed in Figure 4 the κ_0-dependence of the quantity F (in arbitrary units) was obtained. The dependence of the quantity F on parameter η was extracted from the F *vs.* κ_0 and η *vs.* κ_0 curves. In order to determine the values of $F = \frac{k}{2}(1+\eta)^2$ in absolute scale, the datum $k/2 = 4.2 \times 10^{-10}$ cm^3/s, measured for $\eta = 1.6$ at $T = 570$ K, was taken from reference [1]. The check of the Boltzman factors shows that the error related with the scaling of the present results to the value of [1], which was obtained at lower temperature (30 K difference), amounts to 3%.

3 Data analysis and results

The calculated absolute values $F = \frac{k}{2}(1+\eta)^2$ in dependence on the ratio η are given in Figure 5. Fitting these data to a second order polynomial with three parameters (see Eq. (4)), in order to get the values for the rate coefficients k_1, k_2 and k_3 is not sufficiently accurate. This inaccuracy especially concerns k_3, *i.e.*, the intercept of the second order polynomial fit with the ordinate. Namely, the measurements were performed for η values being in the range between 0.6 and 1.75, which is quite apart from the origin. Thus, the determination of the fit parameter is attempted in the region far from the range covered by the experimental data. The best numerical fit to a second order polynomial, yields the values $(18 \pm 2) \times 10^{-10}$ cm^3/s and $(5 \pm 1.5) \times 10^{-10}$ cm^3/s for the rate coefficients k_1 and k_2, respectively, and the non-physical solution $(-2.4 \pm 1) \times 10^{-10}$ cm^3/s for k_3. In order to circumvent the determination of k_3 from the available data set, *i.e.* the fitting to the three parameters, the derivative of the quantity F was made. The least square fit through the derivative $\mathrm{d}F/\mathrm{d}\eta = k_1\eta + k_2$ enables

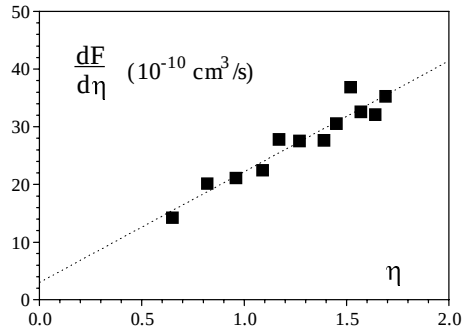

Fig. 6. The derivative of the quantity $F = \frac{k}{2}(1+\eta)^2$ against η. The straight line is the least square fit through the data. The intercept with the ordinate and the slope of the straight line, yield the values for k_2 and k_1, respectively.

more reliable determination of k_1 and k_2. However, in this manner only the upper limit for k_3 could be estimated.

Figure 6 shows the derivative $\mathrm{d}F/\mathrm{d}\eta$ for the mean values of F presented in Figure 5. The least square fit through $\mathrm{d}F/\mathrm{d}\eta$ data yields the straight line parameters, which determine the coefficients k_1 and k_2:

$$k_1 = 2 \times 10^{-9}\ \mathrm{cm}^3/\mathrm{s}, \tag{9}$$

and

$$k_2 = 3.1 \times 10^{-10}\ \mathrm{cm}^3/\mathrm{s}. \tag{10}$$

By varying the data for F and η within their error displayed in Figure 5, the inaccuracy of the above stated values for k_1 and k_2 was found to be 10% and 50%, respectively. Taking into account the error bar of the used value for k, which is reported [1] to be about 30%, the overall uncertainty for the rate coefficients k_1 and k_2 is 40% and 80%, respectively. As for k_3, in the first step one can make the straightforward estimation that $k_3/2$ should be lower than the lowest measured value for F in this experiment, *i.e.*, k_3 should be lower than 5.2×10^{-10} cm^3/s. This conclusion originates from the fact that, since k_i-values are positive, the second order polynomial given by (4) reaches no minimum for positive values of the argument η. With the lowest measured value for F ($\eta = 0.6$) and the lowest values for k_1 and k_2, equation (4) yields the following estimate:

$$k_3 < 3 \times 10^{-10}\ \mathrm{cm}^3/\mathrm{s}. \tag{11}$$

In principle, the additional data set obtained by use of the $6\mathrm{S}_{1/2} \rightarrow 5\mathrm{D}_{3/2}$ excitation channel could give a more precise result for k_3. Namely, in this case the relevant ratio for application of the presented method would be the ratio $N(6\mathrm{P}_{3/2})/N(6\mathrm{P}_{1/2})$, and the constant term in the expression corresponding to equation (4) would be the rate coefficient k_1. Therefore, in the case of the $6\mathrm{S}_{1/2} \rightarrow 5\mathrm{D}_{3/2}$ excitation, one can expect reliably determined values for k_2 and k_3, and an estimate for k_1. Unfortunately, it was shown that the results obtained by using the $6\mathrm{S}_{1/2} \rightarrow 5\mathrm{D}_{3/2}$ excitation pathway cannot be used for the evaluation. First of all, in contrast to $\eta = N(6\mathrm{P}_{1/2})/N(6\mathrm{P}_{3/2})$, the ratio $N(6\mathrm{P}_{3/2})/N(6\mathrm{P}_{1/2})$ can be changed in a narrow region (in principle, between 0.11 and 0.5). Furthermore, the oscillator strength of the $6\mathrm{S}_{1/2} \rightarrow 5\mathrm{D}_{3/2}$ is smaller than that of the used $6S_{1/2} \rightarrow 5D_{5/2}$ transition, and in addition, the gain of the dye laser at the corresponding wavelength 689 nm is a factor of 2 lower than at 685 nm. As a consequence of both these facts, the measurable EP signals appear at the caesium number densities where the relevant fitting parameter is already 0.35. The obtained data are concentrated in a very narrow interval of fitting parameter (between 0.35 and 0.5). The second order polynomial could be fitted through such a "cloud" of the experimental points, but the error bars ($\sim$ 400%) of the resulting rate coefficients make this alternative procedure useless.

The mean Maxwellian relative velocity $v^{\mathrm{rel}}_{\mathrm{Cs-Cs}} = \sqrt{8kT/\pi\mu}$ at $T = 600$ K is 4.4×10^4 cm/s, which gives the following values for the corresponding cross sections: $\sigma_1 = 440 \times 10^{-16}$ cm^2, $\sigma_2 = 70 \times 10^{-16}$ cm^2, and $\sigma_3 < 70 \times 10^{-16}$ cm^2.

4 Discussion and conclusion

The results obtained here and the results of Jabbour *et al.* [2] are listed in Table 1. As mentioned before, the authors in reference [2] measured k_1 and k_2 regarding the fine structure splitting of the Cs $6\mathrm{D}_J$ state, *i.e.* they determined the values $k_i(6\mathrm{D}_{3/2})$ and $k_i(6\mathrm{D}_{5/2})$. Since $k_i = k_i(6\mathrm{D}_{3/2}) + k_i(6\mathrm{D}_{5/2})$, the results from reference [2], listed in Table 1, are recalculated in this way. The data reported here and in reference [2] are obtained at very different temperatures. Therefore, in order to compare these data, the general temperature behaviour of the measured quantities has to be considered.

In the case of $\mathrm{Cs}^*(\mathrm{P}_{1/2}) + \mathrm{Cs}^*(6\mathrm{P}_{1/2})$ collisions, the energy difference ΔE between the final and the initial energy pooling state of colliding two-atom system, is about $+260$ cm^{-1} (f.s. splitting of the 6D state is 43 cm^{-1}). For this endothermic reaction, at given temperature only a fraction of the collisional pairs has sufficient thermal energy to produce the final EP state. At higher temperature this fraction is larger, and the EP cross section is expected to show an increase when temperature increases. For instance, as calculated by Geltman [8], the cross section for the endothermic reaction ($\Delta E = +620$ cm^{-1}) $\mathrm{Na}^*(3\mathrm{P}) + \mathrm{Na}^*(3\mathrm{P}) \rightarrow \mathrm{Na}(3\mathrm{S}) + \mathrm{Na}^{**}(4\mathrm{D})$ is about 3 times higher at $T = 600$ K than at $T = 300$ K. Therefore, it can be understood that the cross section for $Cs^*(P_{1/2}) + Cs^*(6P_{1/2})$ collisions obtained here at 600 K is greater (about two times) than the value reported in [2] for the experimental temperature of 340 K.

In contrast to $\mathrm{Cs}^*(6\mathrm{P}_{1/2}) + \mathrm{Cs}^*(6\mathrm{P}_{1/2})$ collisions, the $\mathrm{Cs}^*(\mathrm{P}_{1/2}) + \mathrm{Cs}^*(\mathrm{P}_{3/2})$ and $\mathrm{Cs}^*(\mathrm{P}_{3/2}) + \mathrm{Cs}^*(6\mathrm{P}_{3/2})$ collisions are the exothermic reactions with energy defects of about -290 cm^{-1} and -850 cm^{-1}, respectively. As calculated by Geltman [8] for the case of the exothermic reaction $\mathrm{Na}^*(3\mathrm{P}) + \mathrm{Na}^*(3\mathrm{P}) \rightarrow \mathrm{Na}(3\mathrm{S}) + \mathrm{Na}^{**}(5\mathrm{S})$, the cross section decreases slowly with the increased temperature,

and, for instance, the corresponding cross section is about 10% lower at 600 K than at 300 K. The same temperature trend can be observed by comparison of the k_3 datum of [2] with the estimated upper limit for k_3 given in this work.

On the basis of the above consideration, and taking into account the experimental errors, one can conclude that the results of the present investigations and the corresponding results for k_1 and k_3 of Jabbour *et al.* [2] are not in contradiction. The value for k_2 is reported for the first time in this work.

The order of magnitude of the measured cross sections, especially concerning the σ_1, indicates that the transition probability for the corresponding energy pooling reaction reaches its maximum at the distances of about 1 nm between colliding atoms. As shown in the case of sodium 3P fine structure mixing induced by collisions with rubidium and caesium atoms [9], this suggests that the investigated energy pooling reactions could be essentially governed by the long-range electrostatic interaction.

The author acknowledges gratefully financial support by the Ministry of Science of Republic of Croatia.

References

1. C. Vadla, K. Niemax, J. Brust, Z. Phys. D **37**, 241 (1996).
2. Z.J. Jabbour, R.K. Namiotka, J. Huennekens, M. Allegrini, S. Milosevic, F. de Tomasi, Phys. Rev. A **54**, 1372 (1996).
3. A.N. Klyucharev, A.V. Lazarenko, Opt. Spectrosc. **32**, 1063 (1972).
4. N.N. Bezuglov, A.N. Klyucharev, V.A. Sheverev, J. Phys. B **20**, 2497 (1987).
5. V.M. Borodin, I.V. Komarov, Opt. Spectrosc. **36**, 145 (1974).
6. T. Yabuzaki, A.C. Tam, M. Hou, W. Happer, S.H. Curry, Opt. Commun. **24**, 305 (1978).
7. K. Niemax, J. Quant. Spectrosc. Radiat. Transfer **16**, 747 (1977).
8. S. Geltman, Phys. Rev. A **40**, 2301 (1989).
9. C. Vadla, M. Movre, V. Horvatic, J. Phys. B: At. Mol. Opt. **27**, 4611 (1994).